Imaging spectrometry for detecting feces and ingesta contamination on poultry carcasses

B. Park, W.R. Windham, K.C. Lawrence, R.J. Buhr and D.P. Smith
USDA, ARS, Richard B. Russell Research Center, Athens, GA 30604-5677, USA.
E-mail: bpark@saa.ars.usda.gov

Introduction

With the implementation of the Hazard Analysis Critical Control Point (HACCP) System,[1] industry was mandated to establish science-based process controls. The detection of fecal and ingesta contamination by visual observation is far from a science-based approach to process control. In addition, there has been a dramatic increase in water usage in most plants as a result of the zero tolerance standard. Plants have nearly doubled their previous water usage and, nationwide, the usage has increased by an estimated two billion gallons.[2] Development of image sensor technology that retains individual carcass inspection for on-line detection of fecal and ingesta contamination, would provide a science-based process control and decrease water usage.

Recently, hyperspectral imaging (or imaging spectrometry) has emerged as a powerful technique in earth remote sensing, but is also being utilised in medical,[3–5] biological,[6–8] agricultural[9–14] and industrial[15–18] areas as well. Hyperspectral imaging is an imaging technique that combines aspects of conventional imaging with spectrophotometry and radiometry. This technique is capable of providing an absolute radiometric measurement over a contiguous spectral range for each and every pixel of an image. Thus, data from a hyperspectral image contains two-dimensional spatial information as well as spectral information. These data can be considered as a three-dimensional "hypercube" which can provide physical and/or chemical information of a material under test. This information can include physical and geometric observations of size, orientation, shape, colour and texture, as well as chemical/molecular information such as water, fat, proteins and other hydrogen-bonded constituents. Hyperspectral imaging is an extremely useful tool to thoroughly analyse the spectra of inhomogeneous materials that contain a wide range of spectral and spatial information. Therefore, it can be an effective technique for identifying surface contaminates on poultry carcasses. The objective of this research is to develop a hyperspectral imaging technique for the identification of fecal and ingesta contamination on the surface of poultry carcasses.

Materials and methods

Materials

A total of 80 fecal and ingesta samples from 20 poultry carcasses were obtained from a local broiler house, transported to the grow-out facilities located at Athens, Georgia and held for four days. Many

Near Infrared Spectroscopy: Proceedings of the 10th International Conference

random variables affect the fecal and ingesta content of the digestive tract. However, the variables were fixed as follows. The samples used were six-week old male birds. Corn with soybean meal were fed for diet. Food and water were withdrawn eight hours and four hours prior to processing the birds, respectively.

The feeding regime was scheduled for meal feeding to provide a consistent amount of fecal material in the digestive tract among the birds. The birds were stunned (12 VAC), bled for 90 s, scalded at 57.5°C (hard scald) for 2 min and picked in the Russell Research Center pilot scale processing facility. In order to collect feces and ingesta, four replicates of 20 birds were processed and eviscerated to obtain fecal materials from the duodenum, ceca, colon and ingesta from the proventriculus and gizzard.

Methods

A transportable hyperspectral imaging system was designed to provide both portability and flexibility in positioning both the lights and the camera system. The imaging system consists of an imaging spectrograph, a high resolution CCD camera with a 1280 × 1024 pixel resolution, compact C-mount lens, motor for lens motion control, frame-grabber and computer. The prism–grating–prism spectrograph has a nominal spectral range of 400 nm to 900 nm with 6.6 mm axis and attaches to the camera for generating line-scan images. The lighting system consists of a 150-watt quartz halogen DC stabilised fibre-optic illuminator, lamp assembly, fibre-optic cables and 10-inch illuminating size of quartz halogen line lights.

An experiment was conducted to collect hyperspectral images from hard-scald poultry carcasses. Hard scalding removes the skin cuticle, resulting in a white carcass, whereas a soft scald keeps the cuticle intact, resulting in a yellow carcass. Then, fecal and ingesta detection algorithms were developed from uncontaminated and contaminated hard scald carcasses.

To fully characterise the spectral and spatial nature of the hyperspectral imaging system, a full calibration, considering both spectral and spatial information, is required. This allows comparison of images collected from the hyperspectral imaging system with the key wavelengths selected by the visible/NIR reflectance spectrometer. Wavelength calibration was conducted with several laser lights to determine the wavelength value of each vertical pixel in the line-scan camera system. Also, two pencil lights, Mercury–Argon (HgAr) and Krypton (Kr); lasers (543.5, 594, 612, and 632.8 nm) and a spectral lamp power supply were used to identify peaks from known wavelengths.

For the hyperspectral image acquisition, line-scan images were collected using SensiCam software based on the following control settings. Image pixels of high resolution CCD detector were 1280 by 1024; however, actual image size and number of wavelength bands are defined by binning size. For our experiment, four by two binning of the line-scan image created an actual image size of 320 (horizontal) × 340 (vertical) spatial resolution with 512 wavelengths spectral images. In this case, the number of line scans, which depend upon the size of carcass and speed of motor to move lens, was 340. The exposure time and time delay of camera control during image acquisition were 50 msec and zero, respectively. The spectral resolution of hyperspectral images was approximately 0.9 nm and a total file size of each image was 106 Mbytes. Even though scanning time depends on the size of a carcass, the average time to scan the whole carcass was about 34 s.

Hypercube image files were created from line-scan image data using HyperVisual software (ProVision Technologies, Stennis Space Center, MS, USA), which can convert 16 bits of binary data into binary sequence mode data for hyperspectral image processing.

After hyperspectral image files were created, the data size was reduced and the features in the image were enhanced. Dimensionality reduction is an important step in hyperspectral image processing because hyperspectral imaging creates a large amount of data containing enormous spectral and spatial information. Specific wavelength bands of hyperspectral images selected by the results of

spectrophotometry were processed and analysed for finding algorithms to detect fecal and ingesta contamination on the surface of carcasses.

The following four steps of image processing algorithms were executed for the identification of fecal and ingesta contaminated spots on the poultry carcasses. Based on the finding of dominant wavelengths from spectroscopy and band selection from the wavelength calibration, four different wavelength spectral images were selected from hypercube image data. The band selection obtained from wavelength calibration was followed by the calculation of band ratios among the four selected spectral images. After the algorithm to calculate the band ratio of individual spectral image has been conducted, a masking template, which is created by the spectral image from one of the 512 spectral image data, masked the images to eliminate background noise from the carcasses. Finally, the algorithm of histogram stretching was applied to all masked images to visually segregate individual fecal and ingesta contaminants.

Results and discussion

Spectral calibration was conducted to correlate absolute wavelength data from known spectral light sources (HgAr, Kr and Green, Red Laser) to the 512 hyperspectral image bands (1024 pixels with a binning of two) obtained from the CCD sensor. The calibration equation for this hyperspectral imaging system is as follows, where X is the band number ranging from 0 to 511, which can be obtained by hypercube image data converted from line scan image data:

$$\text{Wavelength (nm)} = 380.277 + 0.905\,X + (4.369 \times 10^{-4})\,X^2 - (4.356 \times 10^{-7})\,X^3 (r^2 = 0.9999)$$

Based on the calibration equation, we selected four bands: 58, 143, 190, and 251. Each band corresponded with the wavelength of 434 nm, 517 nm, 565 nm and 628 nm, respectively.

Band-ratio images were calculated from the selected four wavelengths spectral images. Six band-ratio images were obtained from the combination of different wavelength selections. As shown in Figure 1, among band ratio images, the band ratio of 565/517 could identify all different types of feces (duodenum, ceca, colon) and ingesta contaminants including colon feces located at the vent area of

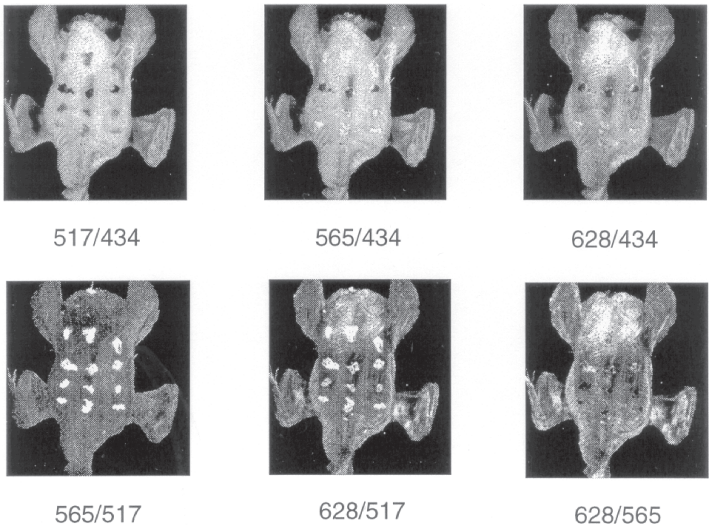

Figure 1. Band ratio images calculated by the combination of two selected spectral images for the identification of feces and ingesta on the poultry carcasses.

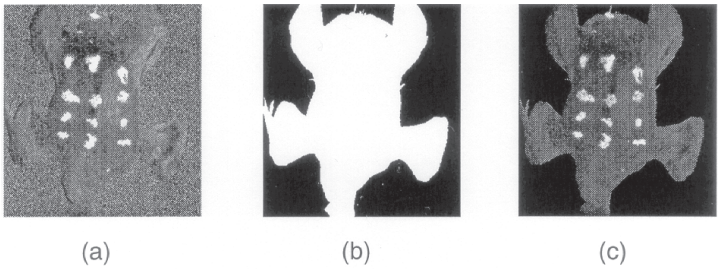

Figure 2. Masking process to eliminate background noise or band ratio processed spectral images. (a) band ratio image (565/517); (b) masking template; (c) band ratio image after masking process.

the tail, which was naturally contaminated during the slaughter of the chicken. The image ratios of 517/434, 565/434 and 628/434 show distinctive ceca (dark spots on the body) contamination.

However, other contaminated spots of duodenum, colon and ingesta were not readily apparent. Even though the ratio image of 628/517 shows contaminated spots on the body, other white spots under the wings and the area between the legs caused false positive errors for feces from the duodenum. Similarly, as seen on the ratio image of 628/565, false positive spots between the legs on the image were actually caused by cuticles or blood hemorrhages on the skin of a carcass.

The background of the original band ratio image was noisier than the chicken body. To eliminate the noisy background, the masking process was implemented for further image processing to segregate the ratio image of a carcass from the background. Figure 2 shows the band ratio (565/517) image before and after the masking process. It was obvious that the masking process made the spots of contamination on the carcass more visually distinctive. To build a masking template, the single spectral image [Band 257 (634 nm)] was selected from 512 hyperspectral images. The template [Figure 2(b)] was created by thresholding the image by choosing minimum thresholding value as zero and maximum value as120, respectively.

After the masking process was applied to ratio images to eliminate background noises, the histogram stretching algorithm was executed to separate feces and ingesta contaminants from a poultry carcass. Both linear and nonlinear histogram stretching algorithms were tested. As shown in Figure 3, the top center white portion of vent area indicates natural contamination of colon feces the second row represents duodenum feces, the third row repersents cecal feces, the fourth row represents colon feces and

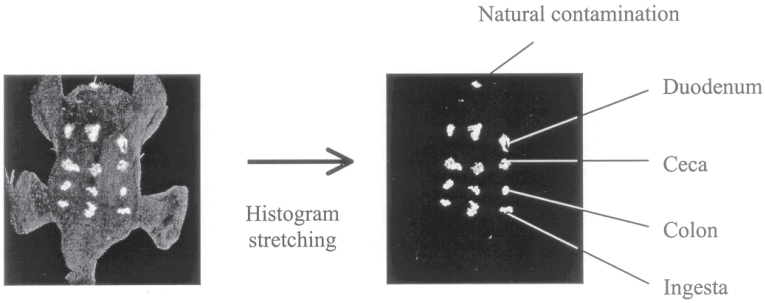

Figure 3. Histogram stretching to separate feces and ingesta from the carcass.

the fifth layer (bottom) represents ingesta contaminants, respectively. The parameter values of histogram stretching algorithm for the sample in Figure 3 were determined as follows: minimun input 1.28; maximum input 1.60; minimum output 0.75; maximum output 2.38.

Conclusions

A hyperspectral imaging system, designed and constructed for this study, provided high resolution multiple spectral images. In conjunction with image processing algorithms (band ratio, histogram stretching, thresholding), the hyperspectral imaging system is an effective technique for the identification of fecal and ingesta contaminants on poultry carcasses. Spectral image band ratio of 565 to 517 performed very well for identification of both feces (duodenum, ceca, colon) and ingesta. Further research into the development of classification algorithms of individual feces and ingesta will enable us to implement a hyperspectral imaging system for HACCP application. Also, the algorithms developed in this study can be effective for the selective multispectral imaging system, in conjunction with batch image-processing algorithms for the real-time, on-line poultry processing applications. By implementing hyperspectral/multispectral imaging techniques, all fecal and ingesta contaminated carcasses can be removed before the chiller tank to prevent cross-contamination at the chiller.

However, even though the hyperspectral imaging technique performed very well, the samples used in this study were limited and different sample conditions need to be considered for the robustness of the system. Therefore, different diet feeding studies should be conducted to investigate the effect of feed ingredients used in broiler finishing diets on the vis/NIR fecal/ingesta spectra and hyperspectral images of contaminated and uncontaminated carcasses, because this is an important factor to select the optimum wavelength to differentiate the location of each feces and ingesta in the digestive tracts of poultry birds.

References

1. USDA, *Fed. Reg*. **61,** 28805 (1996).
2. F.T. Jones, *FSIS Poultry* **6,** 38 (1999).
3. R.M. Levenson, E.S. Wachman, W. Niu and D.L. Farkas, *Proc. SPIE.* **3438,** 300 (1998).
4. M.A. Afromowitz, J.B. Callis, D.B. Heimbach, L.A. DeSoto and M.K. Norton, *IEEE Trans. on Biomedical Engineering* **35,** 842 (1988).
5. C.C. Hoyt, R.R. Richards-Kortum, B. Costello, B.A. Sacks, C. Kittrell, N.B. Ratliff, J.R. Kramer and M.S. Field, *Lasers in Surgery and Medicine* **8N,** 9 Jan (1988).
6. L. Chaerle and D.V.D. Straeten, *Biochemica et. Biophysica Acta* **1519,** 153 (2001).
7. E.B. Chase, C.E. Cooper, D.T. Delpy and E.O.R. Reynolds, *Phil. Trans. R. Soc. Lond.* **B352,** 649 (1997).
8. P. Robert, D. Bertrand, M.F. Devaux and A. Sire, *Anal. Chem*. **64,** 664 (1992).
9. J. Heitschmidt, M. Lanoue, C. Mao and G. May, *Proc. SPIE.* **3544,** 134 (1998).
10. R. Lu, Y.R. Chen, B. Park, and K.H. Choi, *ASAE Technical Paper No.* **993120,** (1999).
11. R. Lu and Y.R. Chen, *Proc. SPIE*. **3544,** 121 (1998).
12. M.S. Borhan, S. Panigrahi, J. Lorenzen and H. Gu, *ASAE Technical Paper No*. **011153,** (2001).
13. A.Y. Muir, I.D.G. Shirlaw and D.C. McRae, *Agricultural Engineer* **Autumn,** 79 (1989).
14. M. Tsuta, J. Sugiyama and Y. Sagara, *J. Agric. Food Chem* **1,** (2001).
15. C.T. Willoughby, M.A. Folkman and M.A. Figueroa, *Proc. SPIE.* **2599,** 264 (1996)
16. W.F. McClure. *NIR news* **2(2),** 8 (1991).
17. Y. Sakamoto, K. Tajiri, T. Sawai and Y. Aoki, *IEEE Trans. on Geoscience and Remote Sensing* **26(4),** 430 (1988).
18. D. Wienke, W. v. d. Broek, W. Melssen, L. Buydens, R. Feldhoff, T. Huth-Fehre, T. Kantimm, F. Winter and K. Cammann, *J. Anal. Chem.* **354,** 823 (1996).